

An Alpha-glucosidase Enzyme Inhibitor Cycloeucalenol from *Sarcolobus globosus* Unveiled through *In vitro* and Computational Analysis

Md. Nazmul Islam¹, Utpal Kumar Karmakar¹, Hiron Saraj Devnath¹,
Md. Amirul Islam¹, Md. Iqbal Ahmed¹, Partha Biswas²,
Masami Ishibashi³ and Samir Kumar Sadhu¹

¹Pharmacy Discipline, Life Science School, Khulna University, Khulna 9208, Bangladesh

²Department of Genetic Engineering and Biotechnology, Jashore University of Science and Technology,
Jashore 7408, Bangladesh

³Laboratory of Natural Products Chemistry, Graduate School of Pharmaceutical Sciences, Chiba University,
Chiba 260-8675, Japan

(Received: June 24, 2024; Accepted: January 28, 2025; Published (web): May 11, 2025)

ABSTRACT: *Sarcolobus globosus* is a medicinal plant grown in the Sundarbans, exhibiting a spectrum of pharmacological properties. This study was devised to scrutinize the potential antidiabetic attributes intrinsic to *S. globosus* leaves. In the oral glucose tolerance test (OGTT), the extract displayed a dose-dependent reduction in blood glucose levels compared to the standard glibenclamide. The extract also demonstrated a notable suppression of the alpha-glucosidase enzyme ($IC_{50} = 0.407$ mg/ml), juxtaposed against the efficacy of the established standard voglibose ($IC_{50} = 0.329$ mg/ml). Cycloartane triterpene, identified as cycloeucalenol, was isolated, exhibiting an IC_{50} of 0.423 mg/ml. Cycloeucalenol was subjected to MD analysis against the protein model (PDB ID: 3A4A), revealing a binding affinity of -9.4 kcal/mol, exceeding that of voglibose (-6.1 kcal/mol), and closely approximating the binding affinity of acarbose (-9.7 kcal/mol). Afterward, cycloeucalenol and acarbose were subjected to MDS studies to explore thermal stability. In addition, an ADMET analysis was performed, affirming the oral bioavailability and safety profile of cycloeucalenol.

Key words: *Sarcolobus globosus*, Cycloeucalenol, Antidiabetic, Alpha-glucosidase enzyme inhibition, MDS Study.

INTRODUCTION

Diabetes mellitus constitutes a metabolic anomaly marked by elevated levels of blood glucose (hyperglycemia) due to aberrations in insulin secretion, insulin action or both.¹ Projected figures suggest that the prevalence of diabetes could more than double by 2030.² Individuals afflicted with diabetes experience a spectrum of complications, including renal failure, neurological disorders, multi-organ dysfunction and ultimately, premature mortality.³ Encouragingly, effective management involving glycemic control and lifestyle adjustments

has the potential to mitigate these complications.^{4,5} Despite the availability of preventive measures, the rapid increase in insulin resistance, coupled with significant adverse effects associated with current oral antidiabetic agents such as sulfonylureas and thiazolidinediones, necessitates fresh research into glycemic control strategies with diminished negative repercussions.^{6,7} Risk factors for managing type-2 diabetes include postprandial hyperglycemia, where the alpha-glucosidase enzyme located at the small intestine's brush border plays a pivotal role by catalyzing carbohydrate hydrolysis into simple sugars.^{8,9} The alpha-glucosidase inhibitors reversibly act on that enzyme, consequently delaying the absorption of sugars from the gut and thus way controlling the blood glucose levels.¹⁰ This inhibition

Correspondence to: Samir Kumar Sadhu
E-mail: sksadhu1969@yahoo.com; sksadhu1969@pharm.ku.ac.bd

Dhaka Univ. J. Pharm. Sci. 24(1): 11-28, 2025 (June)
DOI: <https://doi.org/10.3329/dujps.v24i1.82404>

can be beneficial for individuals with diabetes or those at risk of developing the condition. Alpha-glucosidase inhibitors are commonly used as part of diabetes management and can help to control blood sugar levels after meals.¹¹ Some examples of alpha-glucosidase inhibitors include acarbose, voglibose, and miglitol, which are prescription medications, as well as natural compounds found in certain plants and foods.¹² The growing popularity of alpha-glucosidase inhibitors for glycemic control can be attributed to their distinctive properties of safety and tolerability.¹³ Accordingly, the focus has shifted towards exploring natural botanical sources to identify antidiabetic agents with minimal side effects, as evidenced by successes such as the discovery and synthesis of metformin, an alpha-glucosidase inhibitor originated from *Galega officinalis*.¹⁴

Many plant-derived compounds have been used traditionally in medicine for their potential therapeutic benefits. These compounds may interact with target proteins involved in diseases, offering a promising aspect for drug development.¹⁵ By precisely modulating the activity of a specific protein (either binding to the protein's active site or interfering with the protein's structure), drugs can exert a more focused therapeutic effect, potentially leading to better treatment outcomes. Selective compounds are less likely to interact with unintended proteins or systems in the body; therefore, this approach also allows targeted modulation of the biological pathway without affecting unrelated proteins as well as reducing the occurrence of adverse side effects that are commonly associated with less specific drugs.¹⁶ If a selective compound shows better efficacy against specific target protein(s), it can bolster the case for further drug development efforts. Therefore, due to its precision, efficacy, safety and a better understanding of disease biology, selective protein inhibition is crucial in drug discovery.¹⁷

The Sundarbans, situated in the southern part of Bangladesh, represent the world's largest mangrove forest, harboring a diversity of plant species renowned for their medicinal properties. While many

novel compounds have been extracted, a multitude of plants within this forest remain unexplored from a scientific standpoint.¹⁸ In this context, a specimen from the Sundarbans, *Sarcolobus globosus* Wall., belonging to the Asclepiadaceae family, was selected for the assessment of its antidiabetic potential. *S. globosus* is a climber-type plant (5 m long, 5 mm diameter) whose aerial roots are observed at the base, the bark is smooth, leaves are simple, flowers are bisexual and fruits are 5-8 cm in diameter with a light brown color. Locally known as Baolilata, this plant is widely distributed in the Sundarbans, Cox's Bazar, Khulna and Bagerhat districts in Bangladesh.¹⁹ Traditional medicine has historically utilized this plant to treat conditions like rheumatism, dengue and fever.²⁰

Significant therapeutic potentials of this plant have been documented, encompassing activities such as inhibition of the 15-lipoxygenase (15-LOX) enzyme,²¹ neuromuscular blocking effects,²² inhibition of calcium-dependent contractions,²³ cytotoxic properties,²⁴ membrane stabilization, thrombolytic actions,²⁰ and antibacterial attributes²⁵. While new compounds, sarcolobin, and sarcolobone, have been unveiled from the stems,^{21,26} the antidiabetic potentials of this plant remain unexplored. Intriguingly, diabetes is one of the disorders influenced by the 15-LOX enzyme,²⁷ and given that the stem extract demonstrates inhibitory activity against this enzyme,²¹ it holds the potential to contribute to hyperglycemic management. Taking these factors into consideration, the primary objective of this study was to assess the antidiabetic potential of the plant extract and to isolate compound(s) that could serve as therapeutic alternatives for diabetes mellitus.

MATERIALS AND METHODS.

General experimental procedures. ¹H and ¹³C NMR spectra were taken in an ECZ-600 spectrometer (JEOL) at 600 and 150 MHz, respectively. High-resolution mass spectrum was taken using an Exactive mass spectrometer (Thermo Fisher Scientific). Optical rotation was measured with a P-

2200 polarimeter (JASCO). All these experiments were conducted in the laboratory of Natural Products Chemistry, Chiba University, Japan.

Materials. The alpha-glucosidase enzyme from *Saccharomyces cerevisiae* and *p*-nitrophenyl- α -D-glucopyranoside substrate (*p*NPG) were obtained from Sigma-Aldrich, Singapore. Bionime (GM100) blood glucose monitor and Bionime (GM100) test strip were procured from Technokit Healthcare Ltd, Bangladesh. Glibenclamide (Square Pharmaceuticals Ltd, Bangladesh), voglibose (Beximco Pharmaceuticals Ltd, Bangladesh) and silica gel (60-120 mesh) (Loba Chemie Pvt Ltd, India) were used. All chemicals and reagents used in this study were of analytical grade. Both analytical and preparative thin layer chromatography were performed on silica gel 60 F254 (0.25 mm thickness) plates (Merck, Germany).

Plant material. Fresh *S. globosus* leaves were collected from the Karamjal area in the Sundarbans in July 2019. The plant was recognized by an expert at Bangladesh National Herbarium, Dhaka. For future reference, a voucher specimen has been deposited there (specimen no. 46493 DACB).

Extraction. Collected leaves were subjected to shade drying and pulverization. Dry powder (200 gm) was soaked in 90% v/v ethanol in a sealed container, which was kept for 7 days with occasional shaking. After filtration, the residue was subjected to a second extraction for another 7 days. The filtrate from two times extraction was evaporated using a rotary evaporator to get the crude extract (16 gm) with an 8% w/w yield.

Experimental animals. Young Swiss albino mice aged 4-5 weeks with an appropriate average weight of 20-30 gm were used. The mice were obtained from Jahangirnagar University, Bangladesh, and housed under standard environmental conditions in the animal facility of the Pharmacy Discipline. The animals were provided with Icdrr,b formulated rodent food and water ad libitum and acclimatized to laboratory conditions for one week before the experiment. Protocols followed for the animal experiment were approved by the animal ethics

committee of Khulna University, Bangladesh (Ethical approval number: KUAEC-2020/02/03).

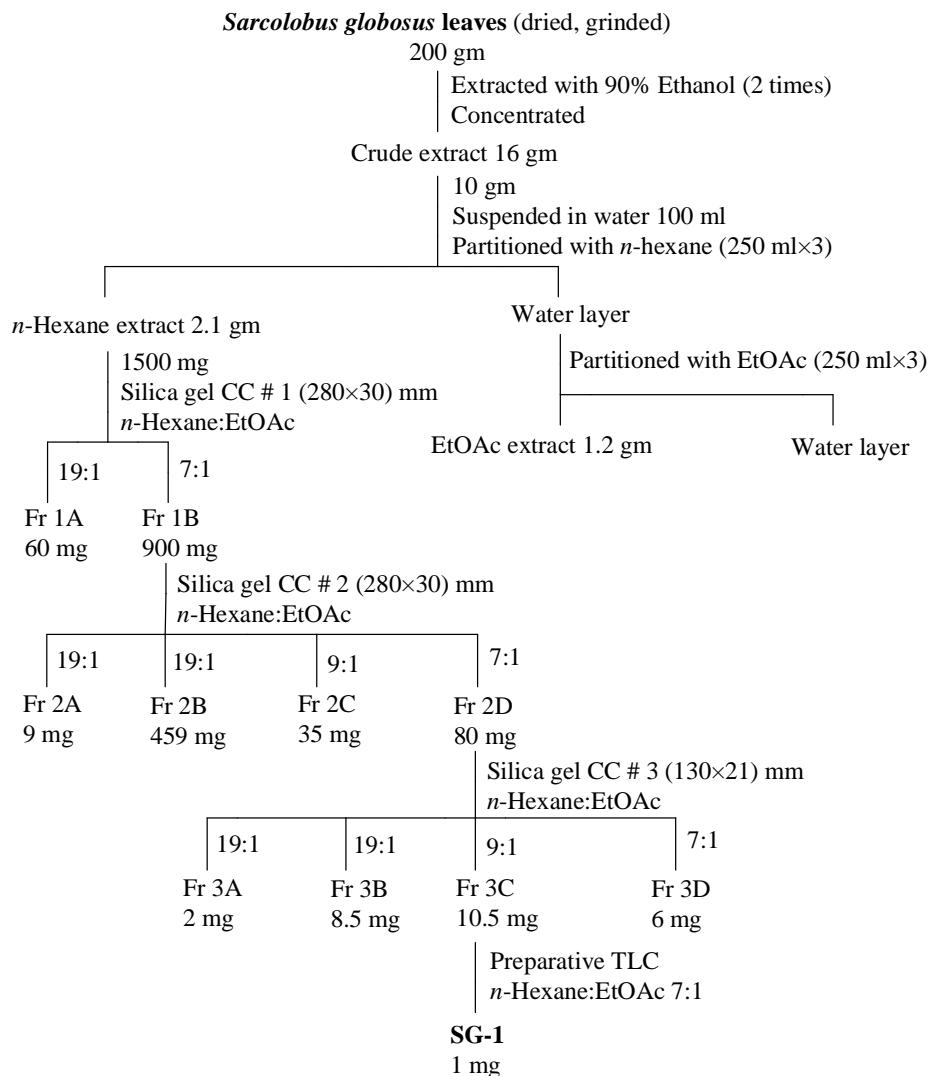
Acute toxicity study. The toxicity of *S. globosus* extract was evaluated using the method of Mahmud and co-workers with slight modifications.²⁸ Fresh young Swiss albino mice were randomly selected and assigned to five groups. The extract was administered via feeding needle at doses of 500, 1000, 2000 and 4000 mg/kg bw, except for the control group, which received 2% v/v tween-80 aqueous solution only. The animals were observed for the first 24 hours and up to 14 days for any signs of change in behavior, mortality, or change in body weight. After the experiment, the mice were euthanized by cervical dislocation and then buried in the soil.

Antihyperglycemic activity test. The antihyperglycemic activity of *S. globosus* leaf extract was evaluated by *in vivo* oral glucose tolerance test (OGTT) according to the method described by Golder and co-workers with slight modifications.²⁹ Experimental mice (n = 5 per group) were grouped into four groups: control group (distilled water 10 ml/kg bw), standard group (glibenclamide 5 mg/kg bw), and two test groups (250 and 500 mg/kg bw). Blood glucose levels of mice in the fasting conditions (only water for at least 12 hours) were measured using a glucometer at 0, 30, 60, 90, 120 and 150 minutes after glucose (2 gm/kg bw) administration.

Isolation of pure compound. The separation of *S. globosus* leaf extract was carried out based on the alpha-glucosidase enzyme inhibitory property. 10 gm of the crude extract was taken and partitioned successively with *n*-hexane (250 ml \times 3), ethyl acetate (EtOAc) (250 ml \times 3), and water. After evaporation, 2.1 gm *n*-hexane extract and 1.2 gm EtOAc extract were obtained, where the alpha-glucosidase enzyme inhibitory activity was found to concentrate in the *n*-hexane extract. *n*-Hexane extract (1500 mg) was then applied to a silica gel column chromatography (CC) (column size (280 \times 30) mm) with the graduated elutes of *n*-hexane:EtOAc 19:1 to 7:1 through which two fractions, fr. 1A and fr. 1B were separated. After spraying 10% H₂SO₄ with heat, fraction 1B showed a major spot on the TLC plate,

and that's why fraction 1B was subjected to a silica gel CC (column size (280×30) mm) from where four fractions, fr. 2A to fr. 2D were obtained with the gradient eluates of *n*-hexane:EtOAc 19:1 to 7:1. Following the major spot, fraction 2D was applied to another silica gel CC (column size (130×21) mm)

with the gradient eluates of *n*-hexane:EtOAc 19:1 to 7:1 and got four fractions, fr. 3A to fr. 3D. Among those, fr. 3C was purified by preparative TLC using *n*-hexane:EtOAc 7:1 solvent system to isolate the compound **SG-1**. The separation flowchart of **SG-1** from *S. globosus* leaf extract is shown in Figure 1.



Inhibitory activity (%) = $(1 - A_s/A_c) \times 100$

Where, A_s = absorbance in the presence of test substance

A_c = absorbance of control.

The IC_{50} values were measured using standard calibration curves.

***In silico* molecular docking (MD) study**

Protein and ligand preparation for MD study.

The protein model PDB ID: 3A4A was selected based on previously conducted studies and downloaded from the protein data bank (<https://www.rcsb.org/>).³¹⁻³³ The model was then prepared by removing water molecules and other ligands, followed by the addition of polar hydrogen atoms.^{34,35} Finally, energy minimization was performed using a Swiss PDB viewer.³⁶ 3D structures of cycloeucalenol (PubChem ID: 101690), voglibose (PubChem ID: 444020) and acarbose (PubChem ID: 444252) were downloaded from PubChem (<https://pubchem.ncbi.nlm.nih.gov/>). Ligand's energy was minimized using a universal force field (UFF) along with the optimization algorithm conjugate gradients and finally, it was converted into PDBQT format in PyRx.^{37,38}

Docking and molecular visualization. Active site residues were selected during MD analysis in PyRx assembled with AutoDock4 and the results were analyzed in LigPlot version 2.2.4.^{37,39} The grid box values selected during the analysis were $x = 20.5376$, $y = -7.1810$ and $z = 18.6343$.

Molecular dynamics simulations (MDS) study. The thermodynamic stability of the selected protein-ligand complexes was analyzed through MDS conducted over 250 ns. The simulations were performed using Schrödinger's Desmond program (v3.6, paid version) on a Linux platform. This study employed the TIP3P water model to simulate the aqueous environment. The system was enclosed in an orthorhombic periodic boundary box with a 10 Å buffer zone around the protein-ligand complex, ensuring an appropriate solvation environment for the simulations. To neutralize the system's electric charge, ions such as Na^+ and Cl^- (from 0.15 M salt)

were randomly distributed throughout the solvent environment. After constructing the solvated protein structures with agonist combinations, the framework was optimized using the OPLS3e force field from the Desmond package. The NPT ensemble was maintained at 300 K and 1 atm (1.01325 bar), followed by a 50 PS equilibration to collect data. The simulation employed the Nose-Hoover thermostat and isotropic pressure coupling. Simulation trajectory analysis was performed using Schrödinger's Maestro program (version 9.5). The proposed model's environment was analyzed using the simulated interaction diagram (SID) from the Desmond module in the Schrödinger suite to evaluate the accuracy of the MD simulation. Protein-ligand complex stability was assessed through parameters such as root-mean-square deviation (RMSD), RMSF- root-mean-square fluctuation, radius of gyration (Rg), solvent-accessible surface area (SASA), molecular surface area (MolSA), polar surface area (PSA), protein-ligand (P-L) interactions and intramolecular bondings.⁴⁰

RMSD analysis. When individual molecules are removed from a system for a defined period, the resulting mean positional deviations are compared to standard measurements using calculated RMSD. Binding RMSD for peptide atomic components, such as carbon atoms, backbone, side chains and heavier atoms was evaluated in this 250 ns MDS study. The binding RMSD reflects how peptides adjust relative to receptor molecules over time, synchronized and assessed for the standard interval. The RMSD for an MD simulation at a given interval, x , is calculated using the following equation (Equation i):

$$RMSD_x = \sqrt{\frac{1}{N} \sum_{i=1}^N (r'_i(t_x) - r_i(t_{ref}))^2} \quad \text{..... (i)}$$

Here, r' represents the position of the chosen molecule in frame x after aligning it to the reference configuration. N is the number of selected molecules, and t_{ref} is the reference time.

RMSF analysis. RMSF primarily monitors structural changes in the transcriptional framework relative to the initial polypeptide configuration. The

following equation is used to calculate RMSF for each amino acid residue (i) during an MD simulation (Equation ii):

$$RMSF_i = \sqrt{\frac{1}{T} \sum_{t=1}^T \langle (r'_i(t) - r_i(t_{ref}))^2 \rangle} \quad (ii)$$

Here, T represents the duration of the simulation trajectories. $r'_i(t)$ is the position of residue i at time t after alignment with the reference structure, $r_i(t_{ref})$ is its position at the reference time and the angle brackets denote the mean distances across all residues.

Post-simulation thermal molecular mechanics-generalized born surface area (MMGBSA) analysis. Thermal MMGBSA of the complexes during the 250 ns simulation was calculated using the thermal_mmgbasa.py tool. The Desmond MD trajectory was divided into 20 discrete frame snapshots and each frame underwent MMGBSA analysis. The ligand was then dissociated from the receptor for further evaluation.

Pharmacokinetic and toxicity (ADME/T) profiling. The pharmacokinetic properties of cycloeucalenol were investigated using SwissADME (<http://www.swissadme.ch>).⁴¹ Toxicological information on cycloeucalenol was obtained from PubChem (<https://pubchem.ncbi.nlm.nih.gov/>).

Statistical analysis. Statistical analysis was performed using Microsoft Excel and Student's unpaired t -test using GraphPad Prism Version 5.0

(GraphPad Software, San Diego, CA, USA). Experimental values were expressed as mean \pm standard deviation (SD), and the mice number in each group was $n = 5$. P values <0.05 were considered statistically significant.

RESULTS AND DISCUSSION

Acute toxicity test. Before the pharmacological test, an acute toxicity study was conducted and the *S. globosus* leaf extract was found to be non-toxic, as evidenced by the absence of mortality and behavioral changes in mice, even at the maximum dose of 4000 mg/kg bw. This result not only demonstrated the safety of this plant but also helped in selecting the doses (250 and 500 mg/kg bw) for the OGTT.

Antihyperglycemic activity test. In the *in vivo* OGTT, *S. globosus* extract suppressed the blood glucose level based on the dose variation (Figure 2) at 60, 90, 120 and 150 minutes after glucose loading. At 60 minutes, the glucose levels decreased to 7.66 ± 0.498 mMol/l ($p = 0.0013$) and 6.76 ± 0.586 mMol/l ($p = 0.0001$), respectively for 250 mg/kg and 500 mg/kg, compared to 9.56 ± 0.723 mMol/l in the control group. Similar trends were observed at subsequent time points, with significant reductions observed at 90 and 150 minutes ($p < 0.05$). These findings indicate the antihyperglycemic potentials of the *S. globosus* extract.

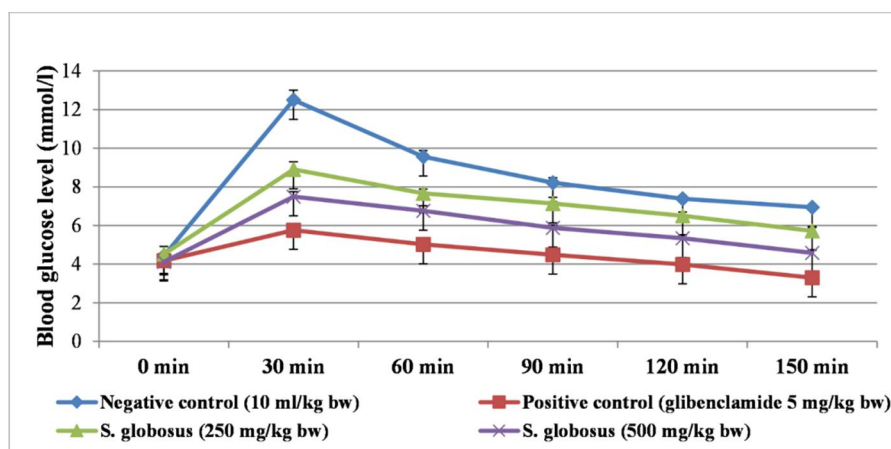


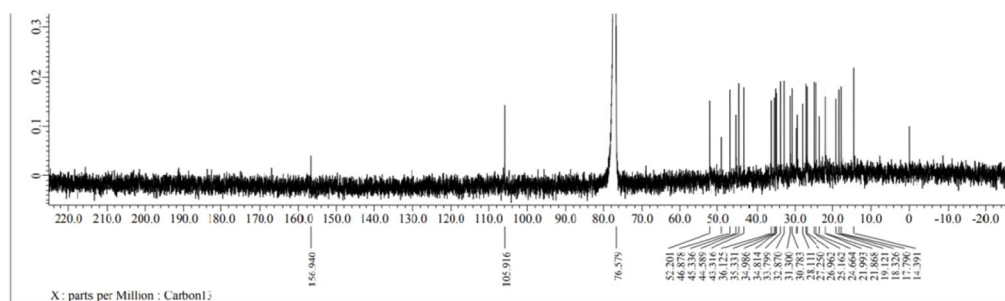
Figure 2. Comparison of blood glucose levels (mmol/l) of *S. globosus* leaf extract in mice over a period in OGTT

Isolation and identification of SG-1.

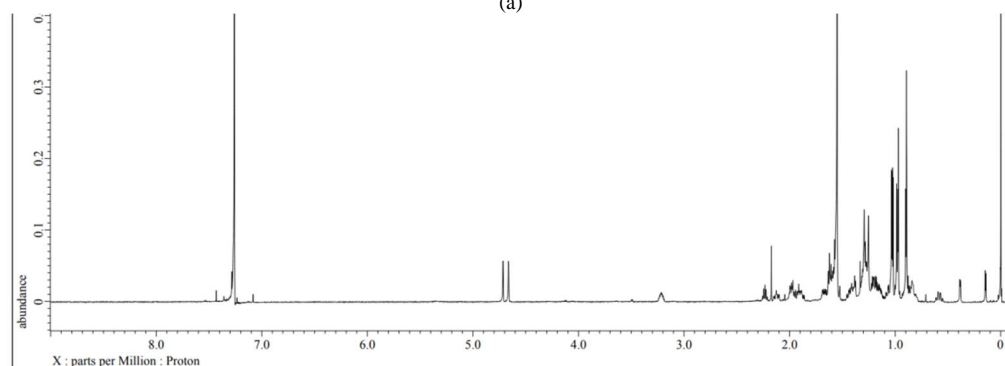
Compound SG-1 (1 mg, purity 99%) was isolated from the *n*-hexane fraction of *S. globosus* leaf extract by activity-guided separation and characterized by detailed 1D and 2D NMR and mass spectroscopy. SG-1 is a colorless amorphous substance, $[\alpha]_D^{24} +42^\circ$ (c 0.1, CHCl_3); $[\alpha]_D +45^\circ$ (CHCl_3) (<https://foodb.ca/compounds/FDB014882>) with R_f value 0.36 at *n*-hexane:EtOAc (5:1) on silica gel TLC.

^{13}C NMR spectrum of **SG-1** (Figure 3a) displayed thirty carbons, of which six were methyl carbons at δ 17.8 (C-18), 18.3 (C-21), 21.9 (C-26),

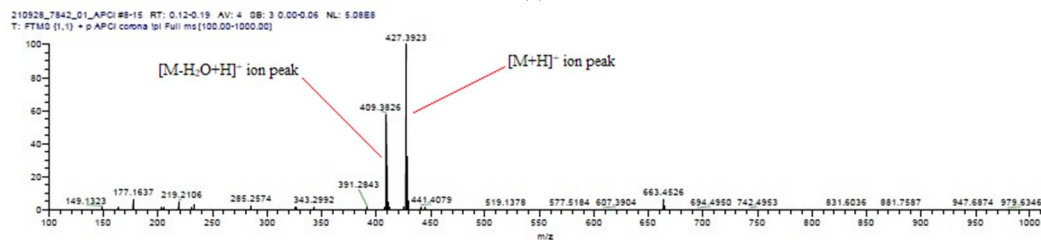
21.9 (C-27), 19.1 (C-29), 14.4 (C-30), twelve were methylene carbons at δ 30.8 (C-1), 34.8 (C-2), 24.7 (C-6), 25.2 (C-7), 26.9 (C-11), 32.8 (C-12), 35.3 (C-15), 28.1 (C-16), 27.3 (C-19), 34.9 (C-22), 31.3 (C-23), 105.9 (C-28), seven were methine carbons at δ 76.6 (C-3), 44.6 (C-4), 43.3 (C-5), 46.9 (C-8), 52.2 (C-17), 36.1 (C-20), 33.8 (C-25) and five were quaternary carbons at δ 23.5 (C-9), 29.5 (C-10), 45.3 (C-13), 48.9 (C-14), 156.9 (C-24). SG-1 has an olefinic bond attached to the 24th carbon which corresponds to peaks at δ 105.9 (C-28) and 156.9 (C-24).



(a)



(b)



(c)

Figure 3. (a) ^{13}C NMR, (b) ^1H NMR, and (c) High-resolution atmospheric pressure chemical ionization mass spectrum (HRAPCIMS) of compound SG-1

In the ^1H NMR spectrum of **SG-1** (Figure 3b), six methyl signals were observed at 0.90 (s, 29-H), 0.90 (d, 5.4, 21-H), 0.96 (s, 18-H), 0.98 (d, 6.0, 30-H), 1.01 (d, 6.0, 26-H), and 1.03 (d, 6.6, 27-H). It showed two olefinic proton signals at δ 4.66 (d, 1.8, 28-H) and 4.70 (br s, 28-H) and a methine proton signal at δ 3.20 (m, 3-H) indicating its attachment to an -OH group. Two methylene proton signals were observed at a very high field at 0.14 (d, 4.2, 19-H)

and 0.38 (d, 4.2, 19-H) suggesting a cyclopropane structure that was joined to cyclohexane at positions C-9 and C-10 (Table 1). HRAPCIMS of SG-1 showed $[\text{M}+\text{H}]^+$ ion peak at 427.3923 (calc. mass 427.3934) and $[\text{M}-\text{H}_2\text{O}+\text{H}]^+$ ion peak at 409.3826 (calc. mass 409.3829) (Figure 3c).⁴² COSY and major HMBC correlations of SG-1 are presented in Figure 4a.

Table 1. ^1H and ^{13}C NMR (δ ppm) assignments of compound SG-1 (Cycloeucalenol) in CDCl_3

Carbon number	^{13}C (150 MHz)	^1H (600 MHz)
C-1	30.8	1.58 (1H, m) 1.28 (1H, m)
C-2	34.8	1.98 (1H, m) 1.41 (1H, m)
C-3	76.6	3.20 (1H, m)
C-4	44.6	1.16 (1H, m)
C-5	43.3	1.20 (1H, m)
C-6	24.7	1.67 (1H, m)
C-7	25.2	0.57 (1H, qd, 12.6, 3.0) 1.06 (1H, qd, 11.4, 3.6) overlapped 1.29 (1H, m)
C-8	46.9	1.59 (1H, m)
C-9	23.5	
C-10	29.5	
C-11	26.9	1.20 (1H, m) 1.96 (1H, m)
C-12	32.8	1.62 (2H, m)
C-13	45.3	
C-14	48.9	
C-15	35.3	1.29 (2H, m)
C-16	28.1	1.29 (1H, m) 1.91 (1H, m)
C-17	52.2	1.62 (1H, m)
C-18	17.8	0.96 (3H, s)
C-19	27.3	0.14 (1H, d, 4.2) 0.38 (1H, d, 4.2)
C-20	36.1	1.40 (1H, m)
C-21	18.3	0.90 (3H, d, 5.4)
C-22	34.9	1.15 (1H, m) 1.58 (1H, m)
C-23	31.3	1.89 (1H, m) 2.12 (1H, ddd, 15.6, 12, 4.8)
C-24	156.9	
C-25	33.8	2.23 (1H, septet, 6.6)
C-26	21.9	1.01 (3H, d, 6.0)
C-27	21.9	1.03 (3H, d, 6.6)
C-28	105.9	4.66 (1H, d, 1.8) 4.70 (1H, br s)
C-29	19.1	0.90 (3H, s)
C-30	14.4	0.98 (3H, d, 6.0)

Comparing the above-mentioned data with published literature, compound SG-1 was identified as a cycloartane triterpene, cycloeucalenol (Figure 4b).⁴³

Alpha-glucosidase enzyme inhibitory activity test. *S. globosus* leaf extract inhibited the enzyme in a concentration-based fashion with an IC_{50} value of 0.407 mg/ml in comparison with standard voglibose (IC_{50} = 0.329 mg/ml). After partitioning, both the *n*-hexane and ethyl acetate fractions were tested, but the *n*-hexane fraction (IC_{50} = 0.479 mg/ml) was found to be more active (IC_{50} = 1.358 mg/ml for ethyl acetate fraction). Cycloeucalenol (SG-1) isolated from the *n*-

hexane fraction inhibited the alpha-glucosidase enzyme with an IC_{50} value of 0.423 mg/ml.

MD study. In the MD studies, binding affinities of cycloeucalenol, voglibose and acarbose were found as -9.4, -6.1, and -9.7 kcal/mol, respectively, with the protein model (PDB ID: 3A4A), and the ligand interactions and binding characteristics are presented in table 2 and figure 5. Two compounds previously isolated from this plant such as sarcobolbin and sarcobolone were also docked and demonstrated lower binding affinities of -7.0 kcal/mol and -8.4 kcal/mol, respectively (Table 2).

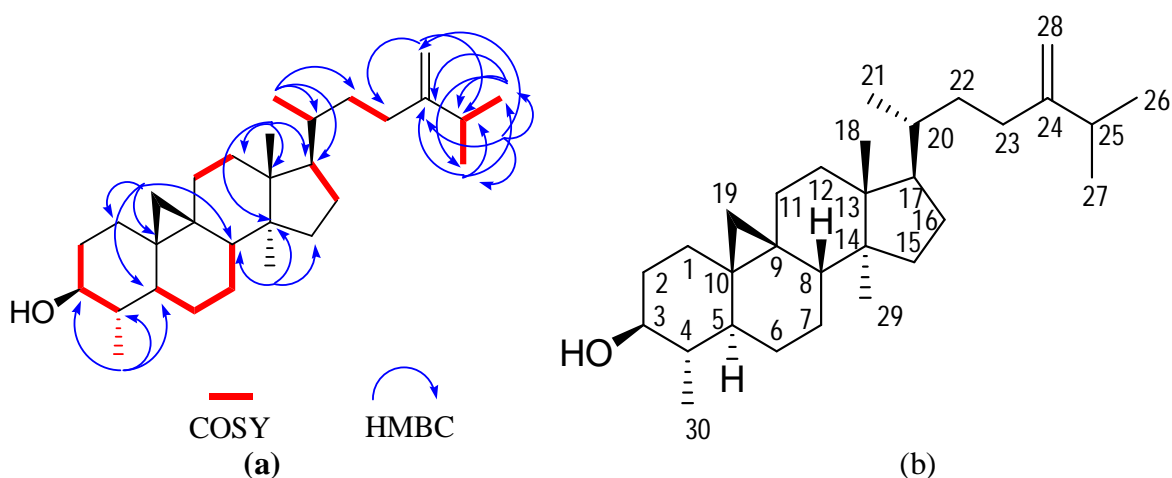


Figure 4. (a) COSY and major HMBC correlations of compound SG-1. (b) Chemical structure of compound SG-1 (Cycloeucalenol)

MDS study.

RMSD analysis. For the 250 ns MDS study, the RMSD values for the two tested ligands acarbose and cycloeucalenol were within the acceptable range. The average RMSD value of acarbose was stable with some fluctuations compared to the value of apo-receptor. Cycloeucalenol showed a considerable RMSD value, which is within the acceptable range compared to the value of the apo-receptor, suggesting the conformational stability of the protein-ligand complex structure presented in figure 6A.

RMSF analysis. Due to the existence of the N- and C-terminal domains, most of the fluctuations were found at the beginning, middle and end of the point protein residues. Consequently, any individual

atom's displacement had a low fluctuation probability for the two ligands, acarbose and cycloeucalenol, compared to the value of the apo-receptor, as illustrated in figure 6B.

Rg analysis. Average Rg values for the ligands acarbose and cycloeucalenol were estimated to be 6.0 and 5.0, respectively, suggesting that upon binding with the selected ligands, the binding sites of the protein do not substantially alter, as presented in figure 6C.

Analysis of SASA, MolSA and PSA. The SASA values for acarbose and cycloeucalenol were between 90 and 440 Å², respectively, suggesting the higher level of interactions in the complex systems presented in figure 6D. In the case of MolSA, both

ligands acarbose and cycloeucaenol possessed the standard Van der Waals surface area (Figure 6E). The targeted protein also showed strong PSA values for both acarbose and cycloeucaenol (Figure 6F).

Analysis of intramolecular bonds. Several features (hydrogen bond, noncovalent bond, water

bridge bond and ionic bond) were used to analyze the interactions between the protein and the selected ligands (acarbose and cycloeucaenol), and the findings demonstrated the stable binding of the ligands with the targeted protein, as depicted in figure 7.

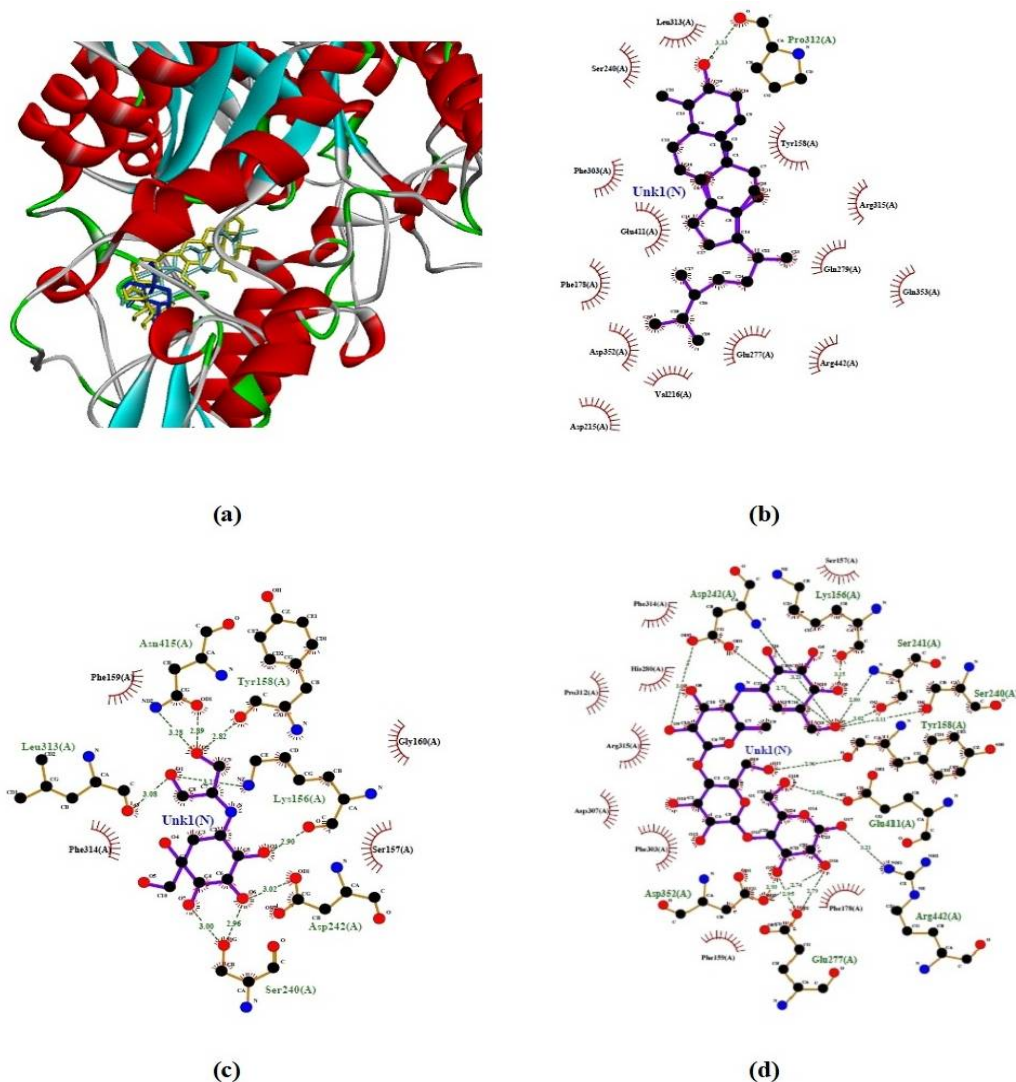


Figure 5. (a) Binding of ligands with alpha-glucosidase enzyme (PDB ID: 3A4A); cycloeucaenol (silver), voglibose (blue), and acarbose (yellow). 2D predicted binding mode of (b) Cycloeucaenol, (c) Voglibose, and (d) Acarbose.

Post-simulation thermal MMGBSA analysis.

The binding free energies of the receptor-ligand complexes during the 250 ns molecular dynamics simulation (MDS) were evaluated using the thermal_mmgsa.py python package. The Desmond MD trajectory was divided into 20 discrete snapshots,

each subjected to MMGBSA analysis. Afterward, the ligand was dissociated from the receptor. Stronger binding between the ligand and receptor resulted in more negative binding free energy values (MMGBSA_dG_Bind_vdW).

Notably, cycloeucaenol showed a binding free energy of –

53.32 kcal/mol, which was similar to the control drug acarbose (−62.20 kcal/mol) (Figure 8).

ADMET profiling analysis. ADMET analysis of the isolated compound cycloeucaenol revealed no mutagenic, carcinogenic or hepatotoxic properties. It is impermeable to the blood-brain barrier (BBB). With a TPSA of 20.23 Å and 5 rotatable bonds, the molecule has a strong support of being utilized orally.

It has only one hydrogen bond donor and acceptor. It is highly lipophilic in nature and poorly soluble in water. Consistent with Lipinski's rule of five, cycloeucaenol is druggable as well as having an excellent absorption pattern (bioavailability score = 0.55). However, in the case of lead-likeness property, it violates two rules mentioned in table 3.

Table 2. Ligand interactions on the active site of alpha-glucosidase enzyme from *S. cerevisiae*.

Ligands	Protein	Binding affinity (kcal/mol)	Interacting amino acids
Acarbose	PDB ID: 3A4A	−9.7	Phe159, Phe178, Glu277, Asp352, Arg442
Voglibose		−6.1	Phe159
SG-1 (Cycloeucaenol)		−9.4	Phe178, Asp215, Val216, Glu277, Asp352, Arg442
Sarcolobin		−7.0	Asp352, Arg442
Sarcolobone		−8.4	Asp352, Arg442

Active site residues of PDB ID: 3A4A are Asp69, Tyr72, His112, Phe159, Phe178, Arg213, Asp215, Val216, Glu277, His351, Asp352, and Arg442.

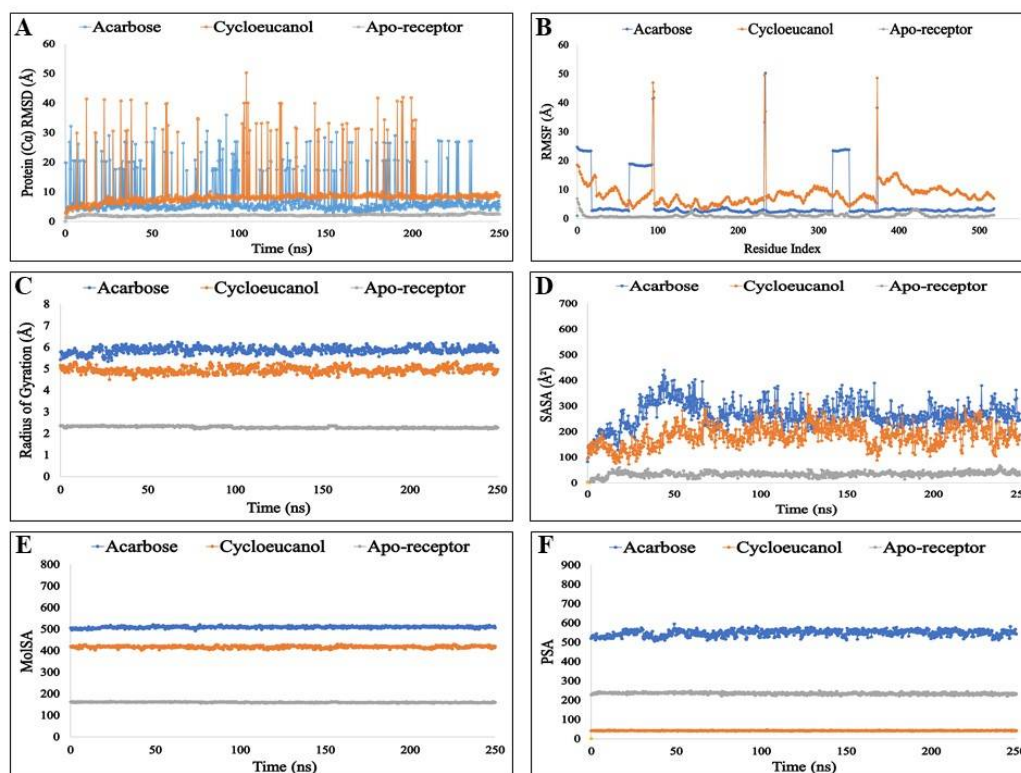


Figure 6. A graphical depiction of the MDS findings over a time span of 250 ns. Here, A displayed the root mean square deviation (RMSD) result; B exhibited the result of root-mean-square fluctuation (RMSF), C denoted the values of the radius of gyration (Rg); D exhibited the result of solvent accessible surface area (SASA); E showed the result of molecular surface area (MolSA) and finally, F denoted the result of polar surface area (PSA). The selected ligands acarbose, cycloeucaenol, and apo-receptor in complex with the protein are represented by green, orange and ash, respectively

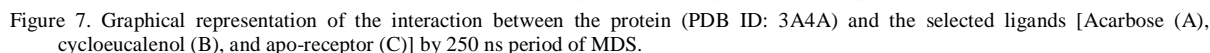


Table 3. Pharmacokinetic profiling (ADMET) of cycloeucalenol.

TPSA-Topological polar surface area; Log P_{o/w}- Predicted octanol/water partition coefficient; BBB- blood-brain barrier; P-gp- P-glycoprotein

For millennia, plants have served as a comprehensive remedy for a diverse array of illnesses, with approximately two-thirds of the world's plant species harboring medicinal properties.⁴⁴ The revolutionary potential of plants and their derivatives lies in their simplicity, safety, eco-friendliness, cost-effectiveness, rapidity and reduced toxicity.⁴⁵ Comprehensive ethnopharmacological surveys across numerous countries have yielded a striking repertoire of plants employed in the treatment of diabetes.⁴⁶ Since diabetes mellitus is one of the major alarming issues worldwide, therefore,

the identification of novel medicinal plants or specific compounds that can effectively address postprandial hyperglycemia without the side effects associated with conventional medications is of paramount importance. In the context of our investigation, we directed our focus to a plant indigenous to the Sundarbans, a member of the Asclepiadaceae family, namely *S. globosus*. The 15-LOX enzyme inhibitory activity of this plant, which has been reported previously,²⁷ reinforced the rationale for exploring its antihyperglycemic potential.

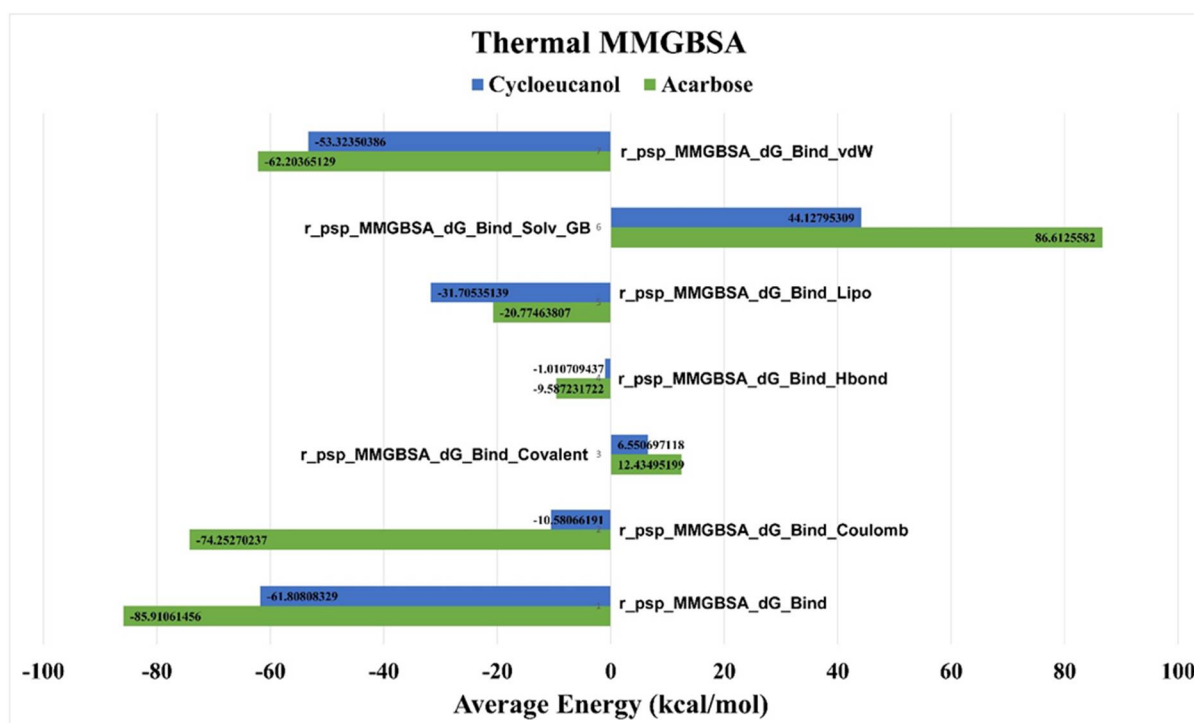


Figure 8. Post-simulation trajectory MMGBSA analysis of cycloeucalenol (blue) and acarbose (green) with the *S. cerevisiae* alpha-glucosidase protein complex (PDB ID: 3A4A)

Prior to delving into pharmacological evaluations, it was important to establish the safety profile of the plant extract. An initial acute toxicity test exhibited no behavioral changes or mortality in treated mice, attesting to the plant's safety. Subsequently, *in vivo* antihyperglycemic evaluations were conducted via OGTT, where the plant extract significantly reduced blood glucose levels. Based on the above finding, further investigation was

necessitated to find out the probable mechanism(s) of lowering blood glucose levels. Therefore, attention was paid to investigating the alpha-glucosidase enzyme inhibitory activity of the leaf extract, where it was found to be active with an IC_{50} value of 0.407 mg/ml compared with standard voglibose (IC_{50} = 0.329 mg/ml). After partitioning of the crude extract, the *n*-hexane fraction showed better activity (IC_{50} = 0.479 mg/ml). Subsequent steps involving column

chromatography and preparative TLC yielded a compound designated as **SG-1**. Compound **SG-1** also exhibited alpha-glucosidase enzyme inhibition (IC_{50} = 0.423 mg/ml) although the crude extract was more potent. This may be due to the synergistic effect of different types of phytochemicals present in the crude extract. Structure determination of **SG-1** was carried out using both 1D and 2D NMR and mass spectroscopy and we found that it was a cycloartane triterpene, identified as cycloeucalenol. Additionally, cycloeucalenol was previously found to be a bioactive antidiabetic compound.⁴⁷ However, the exact mechanism through which this compound exerts the antidiabetic action has not yet been identified. In this study, we attempted to explore the possible mechanism of cycloeucalenol's antidiabetic properties. Notably, several triterpene-like compounds such as ursolic acid, oleanolic acid, and betulinic acid have been reported to target the same binding site on the alpha-glucosidase enzyme as acarbose, exerting enzyme inhibitory effects.⁴⁸ In the context of the above-mentioned findings, the triterpene skeleton of cycloeucalenol might manifest the alpha-glucosidase enzyme inhibitory action in a similar fashion.

In vitro analysis employed voglibose as a standard drug, while it is widely acknowledged that acarbose is the most potent and stable alpha-glucosidase enzyme inhibitor. Hence, *in silico* analysis, acarbose was included as a ligand to assess the comparative efficacy of cycloeucalenol against *S. cerevisiae* alpha-glucosidase (PDB ID: 3A4A). Results indicated that all compounds (cycloeucalenol, voglibose and acarbose) docked within the same binding pocket, with cycloeucalenol exhibiting a binding affinity of -9.4 kcal/mol, surpassing voglibose (-6.1 kcal/mol) and closely approaching acarbose (-9.7 kcal/mol). Cycloeucalenol interacted with amino acid residues Phe178, Asp215, Val216, Glu277, Asp352, and Arg442, while voglibose engaged only with Phe159 at the active site (as illustrated in table 2 and figure 5). Acarbose, on the other hand, interacted with amino acid residues Phe159, Phe178, Glu277, Asp352, and Arg442 at the active site. The presence of common amino acid

residues Phe178, Glu277, Asp352, and Arg442 in both cycloeucalenol and acarbose protein-ligand interactions is notable. Previous investigations have shown that a specific derivative of 3-amino-2,4-diarylbenzo[4,5]imidazo[1,2- α]pyrimidines, 2,4-bis-(4-chloro-phenyl)-benzo[4,5]imidazo[1,2- α]pyrimidin-3-ylamine possesses alpha-glucosidase enzyme inhibitory activity significantly surpassing that of acarbose. MD analysis of that compound demonstrated interactions with amino acid residues Phe303, Tyr158, Asp352, Arg442, Arg315, Val216, Tyr72, His112 and Phe178 at the active site.³² Loss of Asp352 at the protein-ligand interaction site was shown to decrease enzyme inhibitory activity. Therefore, the interaction between Asp352 and cycloeucalenol is likely to assume a pivotal role in the inhibition of the enzyme. Additionally, stabilizing interactions with specific residues like Arg315 and Val216 and hydrophobic interactions with Tyr72, His112, Phe178 and Arg315 significantly contribute to the enzyme inhibitory potency.³² Notably, interactions between cycloeucalenol and Val216 and Phe178 appear to underscore the probable rationale for its superior performance relative to voglibose. Moreover, MD analysis revealed that cycloeucalenol showed a better binding affinity of -9.4 kcal/mol in comparison to the previously isolated two compounds from this plant, sarcolobin (-7.0 kcal/mol) and sarcolobone (-8.4 kcal/mol) (Table 2).

In the 250 ns MDS investigation, RMSD values were within the acceptable range, which typically signifies the average binding positions. The RMSD values for acarbose and cycloeucalenol demonstrated a favorable docking orientation, affirming the absence of disruption in the protein-ligand structure as illustrated in figure 6A. To confirm the dimensional changes of molecules throughout the simulation trajectory, we also computed the SASA of both the protein and ligands.⁴⁹ The SASA outcomes extracted from the MDS trajectory revealed that cycloeucalenol exhibited elevated SASA values (440 Å²) relative to acarbose (90 Å²), as depicted in figure 6D. Furthermore, a higher Rg value suggests a more relaxed molecular packing, while a lower Rg value

signifies a more compact arrangement.⁵⁰ Based on the Rg values, both cycloeucalenol and acarbose, in conjunction with the protein, exhibited standard compactness, as evidenced in figure 6C. Notably, stable bindings were observed between the targeted protein and the selected ligands (acarbose and cycloeucalenol), as shown in figure 7. Both ligands also demonstrated promising values in the MolSA and PSA validation graphs, as portrayed in figures 6E and 6F. Moreover, in the post-simulation binding energy assessment, we found that cycloeucalenol possessed a binding free energy akin to that of the control drug acarbose (Figure 8).

In addition to these considerations, the ADMET analysis of cycloeucalenol suggests its potential as a safe lead candidate for addressing diabetes mellitus, as detailed in table 3. Furthermore, the focal compound of our study, cycloeucalenol, boasts a TPSA of 20.23 Å along with a lower count of rotatable bonds, thereby indicating a strong chance for oral administration.⁵¹ Additionally, a previous study reported the noncytotoxic nature of cycloeucalenol.⁵²

CONCLUSION

The leaf extract of *S. globosus*, a medicinal plant from the Sundarbans, demonstrated dose-dependent hypoglycemic properties by lowering blood glucose levels *in vivo*. The extract also inhibited alpha-glucosidase, an enzyme involved in the metabolism of dietary carbohydrates, *in vitro*. A cycloartane triterpene, cycloeucalenol, isolated from this plant, was found to be a potent inhibitor of the alpha-glucosidase enzyme, with activity comparable to the standard voglibose. Molecular dynamics (MD) analysis supported this finding, showing a stronger binding affinity of cycloeucalenol compared to voglibose and acarbose. In the context of molecular dynamics simulations (MDS), cycloeucalenol exhibited greater structural stability with the alpha-glucosidase enzyme compared to acarbose. Overall, this study suggests that cycloeucalenol could be a promising antidiabetic compound, acting through the alpha-glucosidase enzyme inhibitory pathway.

ACKNOWLEDGMENT

This study was financially supported by the Ministry of Science and Technology (MoST), Bangladesh. The authors would like to thank the authorities of Pharmacy Discipline, Khulna University, for conducting this research project and the experts at Bangladesh National Herbarium, Mirpur, Dhaka, for identifying the plant sample. The authors are also grateful to Dr. Sayaka Kado, Center for Analytical Instrumentation, Chiba University, Japan.

Conflict of interest and consent to publication.

All authors contribute their sincere efforts to carry out the experiments. The authors declare no known conflicts of interest related to this publication, and all authors consented to its publication.

Data availability. All of the experimental data presented here are original and are preserved by the authors. Those will be provided upon request.

CRedit authorship contribution statement.

MNI: Project design, literature search, conduction of experiments, statistical analysis, original manuscript writing and editing. **UKK:** Spectral data analysis and relevant literature search. **HSD:** MD analysis and relevant literature search. **MAI:** Statistical analysis and technical support. **MIA:** Checking of laboratory tests and technical support. **PB:** MDS analysis and graphical presentation. **MNH:** MDS analysis and technical support. **YH:** Conduction of NMR & mass spectroscopy and optical rotation. **MI:** Spectral data analysis, technical support. **SKS:** Project design, idea generation, resources, spectral data analysis, data curation, manuscript writing & editing and overall supervision.

REFERENCES

1. Mellitus, D. 2005. Diagnosis and classification of diabetes mellitus. *Diabetes care* **28**, S5-S10, doi:10.2337/diacare.28.suppl_1.s37.
2. Wild, S., Roglic, G., Green, A., Sicree, R. and King, H. 2004. Global prevalence of diabetes: estimates for the year 2000 and projections for 2030. *Diabetes care*. **27**, 1047-1053, doi:10.2337/diacare.27.5.1047.

3. Smith, Y.A., Adanlawo, I., Oni, O. 2012. Hypoglycaemic effect of saponin from the root of *Garcinia kola* (Bitter kola) on alloxan-induced diabetic rats. *J. drug deliv. ther.* **2**, doi:10.22270/JDDT.V2I6.338.
4. Kidambi, S. and Kotchen, T.A. 2013. Treatment of hypertension in obese patients. *Am. J. Cardiovasc. Drugs* **13**, 163-175, doi:https://doi.org/10.1007/s12020-012-9830-9.
5. Shetty, S., Secnik, K. and Oglesby, A.K. 2005. Relationship of glycemic control to total diabetes-related costs for managed care health plan members with type 2 diabetes. *J. Manag. Care Spec. Pharm.* **11**, 559-564, doi:10.18553/jmcp.2005.11.7.559.
6. Moller, D.E. 2001. New drug targets for type 2 diabetes and the metabolic syndrome. *Nature* **414**, 821-827, doi:10.1038/414821a.
7. Mordarska, K. and Godziejewska-Zawada, M. 2017. Diabetes in the elderly. *Prz. Menopauzalny.* **16**, 38, doi:10.5114/pm.2017.68589.
8. Ceriello, A. 2005. Postprandial hyperglycemia and diabetes complications: is it time to treat? *Diabetes.* **54**, 1-7, doi:https://doi.org/10.2337/diabetes.54.1.1.
9. Mahmood, N. 2016. A review of α -amylase inhibitors on weight loss and glycemic control in pathological state such as obesity and diabetes. *Comp Clin Path.* **25**, 1253-1264, doi:10.1007/s00580-014-1967-x.
10. Campbell, L.K., White, J.R. and Campbell, R.K. 1996. Acarbose: its role in the treatment of diabetes mellitus. *Ann. Pharmacother.* **30**, 1255-1262, doi:10.1177/106002809603001110.
11. Hedrington, M.S. and Davis, S.N. 2019. Considerations when using alpha-glucosidase inhibitors in the treatment of type 2 diabetes. *Expert opinion on pharmacotherapy.* **20**, 2229-2235, doi:https://doi.org/10.1080/14656566.2019.1672660.
12. Dirir, A.M., Daou, M., Yousef, A.F. and Yousef, L.F. 2022. A review of alpha-glucosidase inhibitors from plants as potential candidates for the treatment of type-2 diabetes. *Phytochem. Rev.* **21**, 1049-1079, doi:https://doi.org/10.1007/s11101-021-09773-1.
13. Van de Laar, F.A., Lucassen, P.L., Akkermans, R.P., Van de Lisdonk, E.H., Rutten, G.E. and Van Weel, C. 2005. Alpha-glucosidase inhibitors for type 2 diabetes mellitus. *Cochrane Database Syst. Rev.* doi:10.1002/14651858.CD003639.pub2.
14. Ramya, V., Vembu, S., Ariharasivakumar and G., Gopalakrishnan, M. 2017. Synthesis, characterisation, molecular docking, anti-microbial and anti-diabetic screening of substituted 4-indolylphenyl-6-arylpyrimidine-2-imine derivatives. *Drug Res.* **67**, 515-526, doi:10.1055/s-0043-106444.
15. Atanasov, A.G., Waltenberger, B., Pferschy-Wenzig, E.-M., Linder, T., Wawrosch, C., Uhrin, P., Temml, V., Wang, L., Schwaiger, S. and Heiss, E.H. 2015 Discovery and resupply of pharmacologically active plant-derived natural products: a review. *Biotechnol. Adv.* **33**, 1582-1614, doi:https://doi.org/10.1016/j.biotechadv.2015.08.001.
16. Rask-Andersen, M., Almén, M.S. and Schiöth, H.B. 2011 Trends in the exploitation of novel drug targets. *Nat. Rev. Drug Discov.* **10**, 579-590, doi:https://doi.org/10.1038/nrd3478.
17. Arrowsmith, C.H., Audia, J.E., Austin, C., Baell, J.; Bennett, J., Blagg, J., Bountra, C., Brennan, P.E., Brown and P.J., Bunnage, M.E. 2015. The promise and peril of chemical probes. *Nat. Chem. Biol.* **11**, 536-541, doi:https://doi.org/10.1038/nchembio.1867.
18. Hossain, M.L. 2016. Medicinal activity of *Avicennia officinalis*: evaluation of phytochemical and pharmacological properties. *Saudi J. Med. Pharm. Sci.* **2**, 250-255, doi:10.21276/sjms.2016.2.9.5.
19. Hossain, M. 2015. Handbook of selected plant species of the Sundarbans and the embankment ecosystem. *SDBC-Sundarbans Project implemented by the GIZ and BMZ, Dhaka* **116**.
20. Kuddus, M.R., Aktar, F. and Rashid, M.A. 2011. Polyphenols content, cytotoxic, membrane stabilizing and thrombolytic activities of *Sarcolobus globosus*: A medicinal plant from Sundarban forest. *B LATINOAM CARIBE PL.* **10**, 363-368.
21. Wangenstein, H., Miron, A., Alamgir, M., Rajia, S., Samuelsen, A.B. and Malterud, K.E. 2006. Antioxidant and 15-lipoxygenase inhibitory activity of rotenoids, isoflavones and phenolic glycosides from *Sarcolobus globosus*. *Fitoterapia.* **77**, 290-295, doi:10.1016/j.fitote.2006.03.017.
22. Mustafa, M.R. and Hadi, A.H.A. 1990. Neuromuscular blocking activity of a glycosidic extract of the plant *Sarcolobus globosus*. *Toxicon.* **28**, 1237-1239, doi:10.1016/0041-0101(90)90123-o.
23. Mustafa, M.R. 1993. Inhibition of calcium-dependent contractions of the isolated guinea-pig ileal longitudinal muscle and taenia coli by the total glycosidic extract of the plant *Sarcolobus globosus*. *Toxicon.* **31**, 67-74, doi:10.1016/0041-0101(93)90358-p.
24. Wangenstein, H., Alamgir, M., Rajia, S., Meza, T.J., Samuelsen, A.B. and Malterud, K.E. 2007. Cytotoxicity and brine shrimp lethality of rotenoids and extracts from *Sarcolobus globosus*. *Nat. Prod. Commun.* **2**, doi:https://doi.org/10.1177/1934578X0700200810.

25. Aunjum, A., Biswas, R., Ullah, M.S., Billah, M.M., Islam, M.E. and Islam, K.D. 2019. Bioactivity analysis of *Sarcolobus globosus* Wall., a mangrove plant of the Sundarbans. *J Bangladesh Agril Univ.* **17**, 476-482, doi:10.3329/jbau.v17i4.44608.
26. Wangenstein, H., Alamgir, M., Rajia, S., Samuelson and A.B., Malterud, K.E.J.P.M. 2005. Rotenoids and isoflavones from *Sarcolobus globosus*. *Planta medica.* **71**, 754-758.
27. Sadeghian, H. and Jabbari, A.J.E.O.O.T.P. 2016. 15-Lipoxygenase inhibitors: a patent review. *Expert Opin. Ther. Pat.* **26**, 65-88.
28. Mahmud, I., Zilani, M.N.H., Biswas and N.N., Bokshi, B. 2017. Bioactivities of *Bruguiera gymnorrhiza* and profiling of its bioactive polyphenols by HPLC-DAD. *Clin. Phytoscience.* **3**, 1-11, doi:DOI 10.1186/s40816-017-0048-5.
29. Golder, M., Sadhu, S.K., Biswas, B. and Islam, T. 2020. Comparative pharmacologic profiles of leaves and hypocotyls of a mangrove plant: *Bruguiera gymnorrhiza*. *Adv Tradit Med.* **20**, 395-403, doi:10.1007/s13596-019-00423-8.
30. Islam, M., Devnath, H.S., Medha, M.M., Biswas, R.P., Biswas, N.N., Biswas, B., Sadhu, S.K.J.A.i.T.M. 2022. In silico profiling of analgesic, antidiarrheal and antihyperglycemic properties of *Tetrastigma bracteolatum* (Wall.) leaves extract supported by *in vivo* studies. *Adv. Tradit. Med.* 1-13, doi:https://doi.org/10.1007/s13596-022-00641-7.
31. Lestari, W., Dewi, R.T., Kardono, L.B.S. and Yanuar, A. 2017. Docking sulochrin and its derivative as α -glucosidase inhibitors of *Saccharomyces cerevisiae*. *Indones. J. Chem.* **17**, 144-150, doi:10.22146/ijc.23568.
32. Peytam, F., Takalloobanafshi, G., Saadattalab, T., Norouzbahari, M., Emamgholipour, Z., Moghimi, S., Firoozpour, L., Bijanzadeh, H.R., Faramarzi and M.A., Mojtavavi, S. 2021. Design, synthesis, molecular docking, and *in vitro* α -glucosidase inhibitory activities of novel 3-amino-2,4-diarylbenzo[4,5]imidazo[1,2- α]pyrimidines against yeast and rat α -glucosidase. *Sci. Rep.* **11**, 1-18, doi:https://doi.org/10.1038/s41598-021-91473-z.
33. Ur Rehman, N., Rafiq, K., Khan, A., Ahsan Halim, S., Ali, L.; Al-Saady, N., Hilal Al-Balushi, A., Al-Busaidi, H.K. and Al-Harrasi, A.J.M.D. 2019. α -Glucosidase inhibition and molecular docking studies of natural brominated metabolites from marine macro brown alga *Dictyopteris hoytii*. *Marine Drugs* **17**, 666.
34. Systèmes, D. 2020. BIOVIA, discovery studio visualizer, release 2019. *San Diego: Dassault Systèmes*
35. Devnath, H.S., Ahmed, M.I., Medha, M.M., Islam, M.N., Biswas, R.P.; Islam, M.A. and Sadhu, S.K.J.P.P. 2022. HPLC Analysis and Antimicrobial, Antidiarrheal and antihyperglycemic properties of *Eurya acuminata* along with in silico profiles. *Phytomedicine Plus.* **2**, 100291.
36. Guex, N. and Peitsch, M.C. 1997. SWISS-MODEL and the Swiss-Pdb Viewer: an environment for comparative protein modeling. *electrophoresis.* **18**, 2714-2723, doi:10.1002/elps.1150181505.
37. Dallakyan, S. and Olson, A.J. 2015. Small-molecule library screening by docking with PyRx. In *Chemical biology*; Springer: pp. 243-250.
38. Trott, O. and Olson, A.J. 2010. AutoDock Vina: improving the speed and accuracy of docking with a new scoring function, efficient optimization and multithreading. *J Comput Chem.* **31**, 455-461, doi:10.1002/jcc.21334.
39. Wallace, A.C., Laskowski, R.A. and Thornton, J.M. 1995. LIGPLOT: a program to generate schematic diagrams of protein-ligand interactions. *Protein Eng. Des. Sel.* **8**, 127-134, doi:10.1093/protein/8.2.127.
40. Nur Kabilul Azam, M., Biswas, P., Mohaimenul Islam Tareq, M., Ridoy Hossain, M., Bibi, S., Anisul Hoque, M., Khandker, A., Ashraful Alam, M., Nazmul Hasan Zilani, M., Shahedur Rahman, M., et al. 2024. Identification of antidiabetic inhibitors from *Allophylus villosus* and *Mycetia sinensis* by targeting α -glucosidase and PPAR- γ : *In-vitro*, *in-vivo* and computational evidence. *Saudi Pharm J.* **32**, 101884, doi:10.1016/j.jsps.2023.101884.
41. Daina, A., Michielin and O., Zoete, V.J.S.r. 2017. SwissADME: a free web tool to evaluate pharmacokinetics, drug-likeness and medicinal chemistry friendliness of small molecules. *Scientific reports.* **7**, 1-13, doi:doi: 10.1038/srep42717.
42. Suttiarporn, P., Chumpolsri, W., Mahatheeranont, S.; Luangkamin, S., Teepsawang, S. and Leardkamolkarn, V.J.N. 2015. Structures of phytosterols and triterpenoids with potential anti-cancer activity in bran of black non-glutinous rice. *Nutrients* **7**, 1672-1687, doi:https://doi.org/10.3390/nu7031672.
43. Kikuchi, T., Kadota, S. and Tsubono, K. 1986. Studies on the constituents of orchidaceous Plants. IV.: Proton and carbon-13 signal assignments of cycloeucalenol-type triterpenes from *Nervilia purpurea* Schlechter by two-dimensional nuclear magnetic resonance spectroscopy. *Chem. Pharm. Bull.* **34**, 2479-2486, doi:10.1248/CPB.34.2479.
44. Krishnaiah, D., Sarbatly, R., Nithyanandam, R. 2011. A review of the antioxidant potential of medicinal plant species. *Food Bioprod. Process.* **89**, 217-233, doi:10.1016/j.fbp.2010.04.008.
45. Iqbal, J., Abbasi, B.A., Mahmood, T., Kanwal, S.; Ali, B., Shah, S.A. and Khalil, A.T. 2017. Plant-derived anticancer agents: a green anticancer approach. *Asian Pac. J. Trop. Biomed.* **7**, 1129-1150, doi:https://doi.org/10.1016/j.apjtb.2017.10.016.

46. Telli, A., Esnault, M.-A.; and Khelil, A.O.E.H. 2016. An ethnopharmacological survey of plants used in traditional diabetes treatment in south-eastern Algeria (Ouargla province). *J. Arid Environ.* **127**, 82-92, doi:<https://doi.org/10.1016/j.jaridenv.2015.11.005>.
47. Yumna, M., Arbianti, R., Utami, T.S. and Hermansyah, H. 2018. Effect of mother-in-law's tongue leaves (*Sansevieria trifasciata*) extract's solvent polarity on anti-diabetic activity through *in vitro* α -glucosidase enzyme inhibition test. In Proceedings of the E3S Web of Conferences, p. 03003.
48. López, D., Cherigo, L.; Spadafora, C., Loza-Mejía, M.A., Martínez-Luis, S. 2015. Phytochemical composition, antiparasitic and α -glucosidase inhibition activities from *Pelliciera rhizophorae*. *Chem. Cent. J.* **9**, 1-11, doi:[10.1186/s13065-015-0130-3](https://doi.org/10.1186/s13065-015-0130-3).
49. Elfiky, A.A. and Elshemey, W.M.J.J.O.M.V. 2018. Molecular dynamics simulation revealed binding of nucleotide inhibitors to ZIKV polymerase over 444 nanoseconds. *J. Med. Virol.* **90**, 13-18, doi:<https://doi.org/10.1002/jmv.24934>.
50. Sharif, M., Hossen, M., Shaikat, M.M., Mashuk, F.; Haidary, T., Dey, D., Paul, P.K., Al Azad, S., Al Mazid, M.F. and Badal, M.J.I.J.P.R. 2021. Molecular optimization, docking and dynamic simulation study of selective natural aromatic components to block E2-CD81 complex formation in predating protease inhibitor resistant HCV influx. *Int J Pharm Res.* **13**, 3511-3525, doi:<https://doi.org/10.31838/ijpr/2021.13.02.408>.
51. Veber, D.F., Johnson, S.R., Cheng, H.-Y., Smith, B.R., Ward, K.W. and Kopple, K.D.J.J.o.m.c. 2002. Molecular properties that influence the oral bioavailability of drug candidates. *J. Med. Chem.* **45**, 2615-2623.
52. Adewusi, E.A., Steenkamp, P., Fouche, G. and Steenkamp, V. 2013. Isolation of cycloeucalenol from *Boophone disticha* and evaluation of its cytotoxicity. *Nat. Prod. Commun.* **8**, 1934578X1300800906, doi:<https://doi.org/10.1177/1934578X13008009>.